IEEE Access
Multidisciplinary | Rapid Review | Open Access Journal

Received October 15, 2016, accepted October 28, 2016, date of publication November 2, 2016, date of current version November 18, 2016.

Digital Object Identifier 10.1109/ACCESS.2016.2624561

ESPRIT and Unitary ESPRIT Algorithms for Coexistence of Circular and Noncircular Signals in Bistatic MIMO Radar

GUIMEI ZHENG[1,2], (Student Member, IEEE), JUN TANG[1], (Member, IEEE), and XUAN YANG[1]
[1]Department of Electronic Engineering, Tsinghua University, Beijing 100084, China
[2]Air and Missile Defense College, Air Force Engineering University, Xi'an 710051, China

Corresponding author: G. Zheng (zheng-gm@163.com)

This work was supported in part by the National Natural Science Foundation of China under Grant 61501504, in part by the China Postdoctoral Science Foundation under Grant 2015M581097, and in part by the Natural Science Basic Research Plan in the Shaanxi Province of China under Grant 2016JQ6020.

ABSTRACT In bistatic multiple input multiple output (MIMO) radar, more number of detectable incident signals and a higher angle estimation performance can be obtained by using conjugate estimation of signal parameters via rotational invariance techniques (ESPRITs) with the characteristic of noncircularity. The result is achieved under the assumption that all the received signals are noncircular. When the incident signals are the coexistence of noncircular and circular signals, the conjugate ESPRIT will not valuable. Therefore, this paper proposes a method of the joint of direction of departure (DOD) and direction of arrival (DOA) estimation, which is appropriate for the coexistence of noncircular and circular signals in bistatic MIMO radar. First, the received data model of the bistatic MIMO radar is given. Second, we modify the received signal model by the use of noncircularity characteristic. Third, we derive out the equation of spatially rotational invariant containing the DOD and DOA information. Last, we solve the equation to obtain the DOD and DOA by means of total least squares technology. The proposed algorithm has the three advantages. One is that it has better angle estimation accuracy than that of method which does not use the noncircularity characteristic. Another one is that it has more number of detectable incident signals. The last one is that the more number of noncircular signals, the higher angle estimation accuracy will be. Results from numerical experiments are used to show the effectiveness of our proposed algorithm.

INDEX TERMS Array signal processing, MIMO radar, DOA estimation, ESPRIT, noncircular.

I. INTRODUCTION

Multiple input multiple output (MIMO) radar has received much attention by researchers and industry as its enormous advantages [1]. MIMO radar transmits orthogonal signal waveform through multiple antennas, and receives echoes by the use of multiple antennas. The more phase-center after matched filtering process can be obtained, then the MIMO radar will have larger array aperture than the conventional phased array radar (PAR). Then the MIMO radar has many advantages than PAR in many aspects, for example, target detection, tracking, and imaging, etc [1]–[3]. Angle estimation is always the one of a radar's concerns. So, the algorithms of angle estimation with MIMO radar are developed quickly, such as the references in [4]–[9]. In the following, we give the detailed analysis.

In [4], the classic Capon algorithm, the Amplitude and Phase EStimation (APES) algorithm, and the combination of Capon algorithm and APES (CAPES) are extended to the joint direction of arrival (DOA) and the amplitude of incident signals in monostatic MIMO radar. In [5], the estimation of signal parameters via rotational invariance techniques (ESPRIT) algorithm developed for PAR is extended to the joint estimation of (direction of departure) DOD and DOA with bistatic MIMO radar according to the rotational invariance of the transmitted and received array. But there is a drawback, which is pairing processing between the DODs and DOAs in the case of multi-signal scenario. So, reference [6] uses real-valued processing to realize automatic paring between DODs and DOAs estimation. And it can also improve angle estimation performance under small snapshots. Other classic algorithms for the joint DOD and DOA estimation within bistatic MIMO radar include: the one-dimensional research multiple signal classification (MUSIC) method [7], the combined ESPRIT-MUSIC approach [8],

the alternating projection based maximum likelihood estimation [9], trilinear decomposition-based transmitted angle and received angle estimation [10], the real-valued covariance vector sparsity-inducing estimation [11], and the reduced-dimension MUSIC for angle and array gain-phase error estimation [12].

It is well known that the angle estimation performance and detectable targets can be improved by using noncircularity characteristic of the noncircular signals. Therefore, the conjugate ESPRIT method for MIMO radar, which utilizes the noncircularity characteristics, is developed [13], [14]. In addition, the combined ESPRIT and MUSIC approach in [8] is applied to bistatic [15] and monostatic [16] MIMO radar with the case of noncircular signals. And a sparsity-aware DOA estimation scheme based on a MUSIC-reweighted $L1$ norm penalty for noncircular source is proposed in MIMO radar [17].

The above outstanding works are based on the assumption that all of the received incident signals are noncircular signals. When the received incident signals have circular signals besides the noncircular signals, almost of the above methods will fail. On the other hand, reference [18] solves the problem of coexistence of circular and noncircular signals in PAR. However, the problem of angle estimation in MIMO radar in case of the coexistence of circular and noncircular signals has so far not been derived in the literature. Motivated by the reason, this paper will complete this research. We propose a ESPRIT-like algorithm for the joint DOD and DOA estimation with bistatic MIMO radar under the coexistence of circular and noncircular signals. This paper can also be seen the application of the reference [18] in bistatic MIMO radar. This work appeared in part in the reference [19]. The proposed algorithm has the three advantages: 1) it has better angle estimation accuracy than that of does not use of noncircularity characteristic; 2) it has more number of detectable incident signals; 3) the more number of noncircular signals, the higher angle estimation accuracy will be.

Notations: Superscript $(\cdot)*$, $(\cdot)^T$, and $(\cdot)^H$ denote complex conjugation, transpose, and conjugate transpose, respectively. $\odot$, $\otimes$, and $\oplus$ denote Hadamard-Schur product, Kronecker product, and Khatri-Rao product (columnwise Kronecker product), respectively. Re$\{\cdot\}$ represents the real part of the entity inside. Im$\{\cdot\}$ represents the imaginary part of the entity inside. Tr$\{\cdot\}$ denotes the trace of the entity inside. $\boldsymbol{I}_{MN}$ is a $MN \times MN$ identity matrix. $\boldsymbol{\Pi}_{MN}$ is a $MN \times MN$ exchange matrix. vec$(\cdot)$ denotes vectorization processing. diag$(\cdot)$ denotes diagonalize the vector inside. $\boldsymbol{H} \triangleq \begin{bmatrix} \boldsymbol{A}, \boldsymbol{B}, \boldsymbol{C} \\ \boldsymbol{D}, \boldsymbol{E}, \boldsymbol{F} \end{bmatrix}$ is defined as a 2×3 block matrix, whose elements are also matrices and their dimension must satisfy the construction of a new matrix $\boldsymbol{H}$. rank$(\boldsymbol{R})$ denotes the rank of matrix $\boldsymbol{R}$.

II. SIGNAL MODEL

M transmitted antennas and N received antennas are used in a bistatic MIMO radar. The transmitted and received arrays are set as half-wavelength spacing uniform linear array (ULA). M orthogonal signal waveforms are transmitted by M transmitted antennas, which is expressed as the matrix $\boldsymbol{U} = [\boldsymbol{u}_1^T, \cdots, \boldsymbol{u}_M^T]^T \in \mathbb{C}^{M \times P}$, where $\boldsymbol{U}\boldsymbol{U}^H = \boldsymbol{I}_M$ and P denotes the signal coding length. K far field incident signals impinge on the MIMO radar. The DOD and DOA of incident signal are marked with $\theta \in [-\frac{\pi}{2}, \frac{\pi}{2}]$ and $\phi \in [-\frac{\pi}{2}, \frac{\pi}{2}]$, respectively. Then the echoes of bistatic MIMO radar can be expressed as:

$$\boldsymbol{X}(t) = \boldsymbol{A}_r(\phi) \oplus \text{diag}[\boldsymbol{s}(t)]\boldsymbol{A}_t^T(\theta)\boldsymbol{U} + \boldsymbol{W}(t) \in \mathbb{C}^{MN \times P} \quad (1)$$

where t is 'slow' time index. $\boldsymbol{A}_r(\phi) = [\boldsymbol{a}_r(\phi_1), \cdots, \boldsymbol{a}_r(\phi_K)] \in \mathbb{C}^{N \times K}$ and $\boldsymbol{A}_t(\theta) = [\boldsymbol{a}_t(\theta_1), \cdots, \boldsymbol{a}_t(\theta_K)] \in \mathbb{C}^{M \times K}$ denote the received and transmitted array manifold, in which columns $\boldsymbol{a}_r(\phi_k)$ and $\boldsymbol{a}_t(\theta_k)$ are respectively equal to:

$$\boldsymbol{a}_r(\phi_k) = [1, \exp(j\pi \sin\phi_k), \cdots, \exp(j\pi(N-1)\sin\phi_k]^T \quad (2)$$

$$\boldsymbol{a}_t(\theta_k) = [1, \exp(j\pi \sin\theta_k), \cdots, \exp(j\pi(M-1)\sin\theta_k]^T \quad (3)$$

$\boldsymbol{s}(t) = [s_1(t), \cdots, s_K(t)]^T \in \mathbb{C}^{K \times 1}$ is the reflected signals vector, which contains the radar cross-section (RCS) and Doppler, where $s_k(t) = \beta_k e^{j2\pi f_k t}$, β_k and f_k represent amplitude and Doppler frequency of the k target, respectively. $\boldsymbol{s}(t)$ is set as the mixtures of narrow-band noncircular and circular signals. $\boldsymbol{W}(t) \in \mathbb{C}^{MN \times l}$ is a white Gaussian random process with zero mean and σ_n^2 variance.

Performing matched filtering processing for the received data matrix $\boldsymbol{X}(t)$, namely right-multiplied by the transmitted matrix $\boldsymbol{U}^H$, we can obtain:

$$\begin{aligned} \tilde{\boldsymbol{X}}(t) &= \boldsymbol{X}(t)\boldsymbol{U}^H = \boldsymbol{A}_r(\phi)\text{diag}[\boldsymbol{s}(t)]\boldsymbol{A}_t^T(\theta)\boldsymbol{U}\boldsymbol{U}^H + \boldsymbol{N}(t) \\ &= \boldsymbol{A}_r(\phi)\text{diag}[\boldsymbol{s}(t)]\boldsymbol{A}_t^T(\theta) + \boldsymbol{N}(t) \end{aligned} \quad (4)$$

where $\boldsymbol{N}(t) = \boldsymbol{W}(t)\boldsymbol{U}^H$ denotes the new noise. Performing vectorization operation to Eq. (4)], we can get a MN dimensional vector data:

$$\boldsymbol{y}(t) = \text{vec}\left\{\tilde{\boldsymbol{X}}(t)\right\} = \boldsymbol{A}(\theta, \phi)\boldsymbol{s}(t) + \boldsymbol{n}(t) \in \mathbb{C}^{MN \times 1} \quad (5)$$

where$\boldsymbol{A}(\theta, \phi) = \boldsymbol{A}_t(\theta) \oplus \boldsymbol{A}_r(\phi) \in \mathbb{C}^{MN \times K}$, in which the column vector $\boldsymbol{a}(\theta, \phi) = \boldsymbol{a}_t(\theta) \otimes \boldsymbol{a}_r(\phi)$ is defined as joint transmit-received steering vector. For noise $\boldsymbol{n}(t) = \text{vec}[\boldsymbol{N}(t)]$, it is known from references [3]–[17] that the noise is still a white Gaussian random process.

III. MODIFIED SIGNAL MODEL

We set $K = K_{nc} + K_c$, which K_{nc} denotes the number of noncircular signals and K denotes the number of circular signals. We rewrite the reflected signals as the vector $\boldsymbol{s}(t) = \left[\boldsymbol{s}_{nc}(t)^T, \boldsymbol{s}_c(t)^T\right]^T$, where the vector $\boldsymbol{s}_{nc}(t)$ denotes noncircular signals and $\boldsymbol{s}_c(t)$ denotes circular signals, which

are expressed as

$$\begin{cases} \boldsymbol{s}_{nc}(t) = [s_{nc,1}(t), \cdots, s_{nc,K_{nc}}(t)]^T \\ \boldsymbol{s}_{c}(t) = [s_{c,1}(t), \cdots, s_{c,K_c}(t)]^T \end{cases} \tag{6}$$

Circularity is a characteristic of complex random signals. For a zero-mean complex signal z, the definition of circularity is: $E[zz^H] = \delta^2, E[zz^T] = \rho e^{\eta}\delta^2$, where η is the noncircular phase and $0 \le \rho \le 1$ is the circularity rate. The signal is circular when $\rho = 0$ and noncircular when $0 < \rho \le 1$. Here completely noncircular signals are considered, i.e., $\rho = 1$. According to the above analysis, noncircular signal $s_{nc,i}(t)$ can be written as $s_{nc,i}(t) = \varepsilon_i s_i(t)$, where $\varepsilon_i = e^{j\varphi_i}$ is a complex constant and $s_i(t)$ is a real-valued signal. Therefore, the noncircular signal vector $\boldsymbol{s}_{nc}(t)$ can be rewritten as:

$$\boldsymbol{s}_{nc}(t) = \boldsymbol{\Gamma}\boldsymbol{s}_{\text{real1}}(t) \tag{7}$$

where $\boldsymbol{s}_{\text{real1}}(t) = [s_1(t), \cdots, s_{K_{nc}}(t)]^T$ and $\boldsymbol{\Gamma} = \text{diag}[\varepsilon_1, \cdots, \varepsilon_{K_{nc}}]$. According to the reference [18], one circular signal is divided into the two identical angle real-valued signals, as follows.

$$\boldsymbol{s}_c(t) = [\boldsymbol{s}_{\text{real2}}(t) + j\boldsymbol{s}_{\text{real3}}(t)] = \begin{bmatrix} \boldsymbol{I}_{K_c} j\boldsymbol{I}_{K_c} \end{bmatrix} \begin{bmatrix} \boldsymbol{s}_{\text{real2}}(t) \\ \boldsymbol{s}_{\text{real3}}(t) \end{bmatrix} \tag{8}$$

According to Eqs. (7) and (8), the reflected signals $\boldsymbol{s}(t)$ can be expressed as

$$\begin{aligned} \boldsymbol{s}(t) &= \begin{bmatrix} \boldsymbol{s}_{nc}(t) \\ \boldsymbol{s}_{c}(t) \end{bmatrix} = \begin{bmatrix} \boldsymbol{\Gamma}\boldsymbol{s}_{\text{real1}}(t) \\ \begin{bmatrix} \boldsymbol{I}_{K_c} j\boldsymbol{I}_{K_c} \end{bmatrix} \begin{bmatrix} \boldsymbol{s}_{\text{real2}}(t) \\ \boldsymbol{s}_{\text{real3}}(t) \end{bmatrix} \end{bmatrix} \\ &= \begin{bmatrix} \boldsymbol{\Gamma} & \boldsymbol{0} & \boldsymbol{0} \\ \boldsymbol{0} & \boldsymbol{I}_{K_c} & j\boldsymbol{I}_{K_c} \end{bmatrix} \begin{bmatrix} \boldsymbol{s}_{\text{real1}}(t) \\ \boldsymbol{s}_{\text{real2}}(t) \\ \boldsymbol{s}_{\text{real3}}(t) \end{bmatrix} = \boldsymbol{\Xi}\tilde{\boldsymbol{s}}(t) \end{aligned} \tag{9}$$

where $\boldsymbol{\Xi} \triangleq \begin{bmatrix} \boldsymbol{\Gamma} & \boldsymbol{0} & \boldsymbol{0} \\ \boldsymbol{0} & \boldsymbol{I}_{K_c} & j\boldsymbol{I}_{K_c} \end{bmatrix}$ and $\tilde{\boldsymbol{s}}(t) \triangleq [\boldsymbol{s}_{\text{real1}}(t)^T, \boldsymbol{s}_{\text{real2}}(t)^T, \boldsymbol{s}_{\text{real3}}(t)^T]^T$ a real-valued signal vector. Then the whole received data of Eq. (5) is rewritten as:

$$\begin{aligned} \boldsymbol{y}(t) &= \boldsymbol{A}(\theta,\phi)\boldsymbol{s}(t) + \boldsymbol{n}(t) = \boldsymbol{A}(\theta,\phi)\boldsymbol{\Xi}\tilde{\boldsymbol{s}}(t) + \boldsymbol{n}(t) \\ &= \tilde{\boldsymbol{A}}(\theta,\phi)\tilde{\boldsymbol{s}}(t) + \boldsymbol{n}(t) \end{aligned} \tag{10}$$

where $\tilde{\boldsymbol{A}}(\theta,\phi) = \boldsymbol{A}(\theta,\phi)\boldsymbol{\Xi} \in \mathbb{C}^{MN\times(K_{nc}+2K_c)}$. Eq. (10) indicates that the new form data is similar to the signal model, which $(K_{nc}+2K_c)$ incident noncircular signals impinge into the array of the steering matrix $\tilde{\boldsymbol{A}}(\theta,\phi)$. In the following, we will drive the rotational invariance about the steering matrix $\tilde{\boldsymbol{A}}(\theta,\phi)$ and show the method to estimate the DOD and DOA angles according to the Eq. (10).

IV. PROPOSED ALGORITHM

A. ROTATIONAL INVARIANCE FOR BISTATIC MIMO RADAR

To make full use of noncircularity characteristic of noncircular signal, we compute the conjugation of received data to extend the array aperture (It doubles the array dimension from MN to $2MN$.):

$$\begin{aligned} \boldsymbol{y}_{nc}(t) &= \begin{bmatrix} \boldsymbol{y}(t) \\ \boldsymbol{\Pi}_{MN}\boldsymbol{y}(t)^* \end{bmatrix} = \begin{bmatrix} \tilde{\boldsymbol{A}}(\theta,\phi)\tilde{\boldsymbol{s}}(t) \\ \boldsymbol{\Pi}_{MN}\tilde{\boldsymbol{A}}(\theta,\phi)^*\tilde{\boldsymbol{s}}(t)^* \end{bmatrix} \\ &\quad + \begin{bmatrix} \boldsymbol{n}(t) \\ \boldsymbol{\Pi}_{MN}\boldsymbol{n}(t)^* \end{bmatrix} \\ &= \begin{bmatrix} \tilde{\boldsymbol{A}}(\theta,\phi) \\ \boldsymbol{\Pi}_{MN}\tilde{\boldsymbol{A}}(\theta,\phi)^* \end{bmatrix} \tilde{\boldsymbol{s}}(t) + \begin{bmatrix} \boldsymbol{n}(t) \\ \boldsymbol{\Pi}_{MN}\boldsymbol{n}(t)^* \end{bmatrix} \\ &= \boldsymbol{A}_{nc}(\theta,\phi)\tilde{\boldsymbol{s}}(t) + \boldsymbol{n}_{nc}(t) \end{aligned} \tag{11}$$

where $\boldsymbol{A}_{nc}(\theta,\phi) \in \mathbb{C}^{2MN\times(K_{nc}+2K_c)}$ denotes the joint steering matrix, which can be unwrapped as:

$$\begin{aligned} &\boldsymbol{A}_{nc}(\theta,\phi) \\ &= \begin{bmatrix} \boldsymbol{A}(\theta,\phi)\boldsymbol{\Xi} \\ \boldsymbol{\Pi}_{MN}\boldsymbol{A}(\theta,\phi)^*\boldsymbol{\Xi}^* \end{bmatrix} \\ &= \begin{bmatrix} \boldsymbol{A}_1(\theta,\phi)\boldsymbol{\Gamma}, \boldsymbol{A}_2(\theta,\phi), j\boldsymbol{A}_2(\theta,\phi) \\ \boldsymbol{\Pi}_{MN}\boldsymbol{A}_1(\theta,\phi)^*\boldsymbol{\Gamma}^*, \boldsymbol{\Pi}_{MN}\boldsymbol{A}_2(\theta,\phi)^*, j\boldsymbol{\Pi}_{MN}\boldsymbol{A}_2(\theta,\phi)^* \end{bmatrix} \end{aligned} \tag{12}$$

where $\boldsymbol{A}_1(\theta,\phi)$ and $\boldsymbol{A}_2(\theta,\phi)$ denote the joint transmit-received steering matrix of the first K_{nc} signals and the last K_c signals, respectively, that is $\boldsymbol{A}(\theta,\phi) = [\boldsymbol{A}_1(\theta,\phi)\boldsymbol{A}_2(\theta,\phi)]$. For the upper part of the matrix $\boldsymbol{A}_{nc}(\theta,\phi)$ in Eq. (12), the first and last $(M-1)$ elements of transmitted array has the spatially rotational invariance, mathematically

$$\begin{aligned} &\boldsymbol{A}_{t_1}(\theta,\phi) \\ &= \begin{bmatrix} [\boldsymbol{a}_{t_1}(\theta_1)\otimes\boldsymbol{a}_r(\phi_1), \cdots, \boldsymbol{a}_{t_1}(\theta_{K_{nc}})\otimes\boldsymbol{a}_r(\phi_{K_{nc}})]\boldsymbol{\Gamma}, \\ [\boldsymbol{a}_{t_1}(\theta_{K_{nc}+1})\otimes\boldsymbol{a}_r(\phi_{K_{nc}+1}), \cdots, \boldsymbol{a}_{t_1}(\theta_K)\otimes\boldsymbol{a}_r(\phi_K)], \\ j[\boldsymbol{a}_{t_1}(\theta_{K_{nc}+1})\otimes\boldsymbol{a}_r(\phi_{K_{nc}+1}), \cdots, \boldsymbol{a}_{t_1}(\theta_K)\otimes\boldsymbol{a}_r(\phi_K)] \end{bmatrix} \end{aligned} \tag{13}$$

$$\begin{aligned} &\boldsymbol{A}_{t_2}(\theta,\phi) \\ &= \begin{bmatrix} [\boldsymbol{a}_{t_2}(\theta_1)\otimes\boldsymbol{a}_r(\phi_1), \cdots, \boldsymbol{a}_{t_2}(\theta_{K_{nc}})\otimes\boldsymbol{a}_r(\phi_{K_{nc}})]\boldsymbol{\Gamma}, \\ [\boldsymbol{a}_{t_2}(\theta_{K_{nc}+1})\otimes\boldsymbol{a}_r(\phi_{K_{nc}+1}), \cdots, \boldsymbol{a}_{t_2}(\theta_K)\otimes\boldsymbol{a}_r(\phi_K)], \\ j[\boldsymbol{a}_{t_2}(\theta_{K_{nc}+1})\otimes\boldsymbol{a}_r(\phi_{K_{nc}+1}), \cdots, \boldsymbol{a}_{t_2}(\theta_K)\otimes\boldsymbol{a}_r(\phi_K)] \end{bmatrix} \end{aligned} \tag{14}$$

where $\boldsymbol{a}_{t_1}(\theta)$ and $\boldsymbol{a}_{t_2}(\theta)$ denote the steering vectors of the first and last $(M-1)$ elements of the transmitted array. From Eqs. (13) and (14), we know that there is a rotational invariance between the matrix $\boldsymbol{A}_{t_1}(\theta,\phi)$ and the matrix $\boldsymbol{A}_{t_2}(\theta,\phi)$, as follows.

$$\boldsymbol{A}_{t_2}(\theta,\phi) = \boldsymbol{A}_{t_1}(\theta,\phi)\boldsymbol{\Phi}_\theta \tag{15}$$

where $\boldsymbol{\Phi}_\theta = \text{diag}[e^{j\pi\sin\theta_1}, \cdots, e^{j\pi\sin\theta_K}, e^{j\pi\sin\theta_{K_{nc}+1}}, \cdots, e^{j\pi\sin\theta_K}]$, which includes the DODs of $(K_{nc}+2K_c)$ signals. In addition, a compact matrix form can be used to illustrate Eqs. (13) and (14), as follows.

$$\begin{aligned} \boldsymbol{A}_{t_1}(\theta,\phi) &= [\boldsymbol{O}_1^\theta\boldsymbol{A}_1(\theta,\phi)\boldsymbol{\Gamma}, \boldsymbol{O}_1^\theta\boldsymbol{A}_2(\theta,\phi), \boldsymbol{O}_1^\theta j\boldsymbol{A}_2(\theta,\phi)] \\ &= \boldsymbol{O}_1^\theta[\boldsymbol{A}_1(\theta,\phi)\boldsymbol{\Gamma}, \boldsymbol{A}_2(\theta,\phi), j\boldsymbol{A}_2(\theta,\phi)] \\ &= \boldsymbol{O}_1^\theta\boldsymbol{A}(\theta,\phi)\boldsymbol{\Xi} \end{aligned} \tag{16}$$

$$\begin{aligned} \boldsymbol{A}_{t_2}(\theta,\phi) &= [\boldsymbol{O}_2^\theta\boldsymbol{A}_1(\theta,\phi)\boldsymbol{\Gamma}, \boldsymbol{O}_2^\theta\boldsymbol{A}_2(\theta,\phi), \ \boldsymbol{O}_2^\theta j\boldsymbol{A}_2(\theta,\phi)] \\ &= \boldsymbol{O}_2^\theta[\boldsymbol{A}_1(\theta,\phi)\boldsymbol{\Gamma}, \boldsymbol{A}_2(\theta,\phi), j\boldsymbol{A}_2(\theta,\phi)] \\ &= \boldsymbol{O}_2^\theta\boldsymbol{A}(\theta,\phi)\boldsymbol{\Xi} \end{aligned} \tag{17}$$

where the selection matrices $\boldsymbol{O}_1^\theta$ and $\boldsymbol{O}_2^\theta$ equal $\boldsymbol{O}_1^\theta = [\boldsymbol{I}_{(M-1)N}\boldsymbol{0}_{(M-1)N\times N}]$, $\boldsymbol{O}_2^\theta = [\boldsymbol{0}_{(M-1)N\times N}\boldsymbol{I}_{(M-1)N}]$, respectively. Substituting Eqs. (16) and (17) into (15), we have

$$\boldsymbol{O}_2^\theta \boldsymbol{A}(\theta,\phi)\boldsymbol{\Xi} = \mathrm{O}_1^\theta \boldsymbol{A}(\theta,\phi)\boldsymbol{\Xi}\boldsymbol{\Phi}_\theta \tag{18}$$

Similar to the result of Eq. (18), for the under part of Eq. (12), the following rotational invariance equation holds.

$$\boldsymbol{O}_2^\theta \boldsymbol{\Pi}_{MN}\boldsymbol{A}(\theta,\phi)^*\boldsymbol{\Xi}^* = \boldsymbol{O}_1^\theta \boldsymbol{\Pi}_{MN}\boldsymbol{A}(\theta,\phi)^*\boldsymbol{\Xi}^*\boldsymbol{\Phi}_\theta \tag{19}$$

Combining Eq. (18) and Eq. (19), we can obtain

$$\begin{aligned}&(\boldsymbol{I}_2 \otimes \boldsymbol{O}_2^\theta)\begin{bmatrix}\boldsymbol{A}(\theta,\phi)\boldsymbol{\Xi}\\ \boldsymbol{\Pi}_{MN}\boldsymbol{A}(\theta,\phi)^*\boldsymbol{\Xi}^*\end{bmatrix}\\ &\quad = (\boldsymbol{I}_2 \otimes \boldsymbol{O}_1^\theta)\begin{bmatrix}\boldsymbol{A}(\theta,\phi)\boldsymbol{\Xi}\\ \boldsymbol{\Pi}_{MN}\boldsymbol{A}(\theta,\phi)^*\boldsymbol{\Xi}^*\end{bmatrix}\boldsymbol{\Phi}_\theta\end{aligned} \tag{20}$$

Define the selection matrices $\boldsymbol{J}_1^\theta$ and $\boldsymbol{J}_2^\theta$ as $\boldsymbol{J}_1^\theta \triangleq (\boldsymbol{I}_2 \otimes \boldsymbol{O}_1^\theta) = \boldsymbol{I}_2 \otimes [\boldsymbol{I}_{(M-1)N}\boldsymbol{0}_{(M-1)N\times N}]$ and $\boldsymbol{J}_2^\theta \triangleq (\boldsymbol{I}_2 \otimes \boldsymbol{O}_2^\theta) = \boldsymbol{I}_2 \otimes [\boldsymbol{0}_{(M-1)N\times N}\boldsymbol{I}_{(M-1)N}]$, respectively, then we have the rotational invariance equation.

$$\boldsymbol{J}_2^\theta \boldsymbol{A}_{nc}(\theta,\phi) = \boldsymbol{J}_1^\theta \boldsymbol{A}_{nc}(\theta,\phi)\boldsymbol{\Phi}_\theta \tag{21}$$

Similar to the result of Eq. (21), another rotational invariance equation with the received array can be obtained, as follows.

$$\boldsymbol{J}_2^\phi \boldsymbol{A}_{nc}(\theta,\phi) = \boldsymbol{J}_1^\phi \boldsymbol{A}_{nc}(\theta,\phi)\boldsymbol{\Phi}_\phi \tag{22}$$

where $\boldsymbol{\Phi}_\phi = \mathrm{diag}[e^{j\pi\sin\phi_1}, \cdots, e^{j\pi\sin\phi_K}, e^{j\pi\sin\phi_{K_{nc}+1}}, \cdots, e^{j\pi\sin\phi_K}]$, which includes the DOAs of $(K_{nc}+2K_c)$ signals. The selection matrices are equal to $\boldsymbol{J}_1^\phi = \boldsymbol{I}_{2M} \otimes [\boldsymbol{I}_{(N-1)}\boldsymbol{0}_{(N-1)\times 1}]$ and $\boldsymbol{J}_2^\phi = \boldsymbol{I}_{2M} \otimes [\boldsymbol{0}_{(N-1)\times 1}\boldsymbol{I}_{(N-1)}]$.

B. ESPRIT AND UNITARY ESPRIT FOR DOD AND DOA ESTIMATION

1) ESPRIT

Let $\boldsymbol{Y}$ denotes a matrix consisting of L snapshots of received data $\boldsymbol{y}_{nc}(t_l)$. Then we calculate the covariance matrix by using maximum likelihood, i.e. $\hat{\boldsymbol{R}} = \boldsymbol{Y}\boldsymbol{Y}^H/L$. Let $\boldsymbol{E}_S$ denotes the signal subspace. In the following, we give the analysis about signal subspace dimension. We define a new matrix constructed by the upper part of $\boldsymbol{A}_{nc}(\theta,\phi)$ in Eq. (12):

$$\boldsymbol{A}_{nc}^{\mathrm{up}}(\theta,\phi) \triangleq [\boldsymbol{A}_1(\theta,\phi)\boldsymbol{\Gamma}, \boldsymbol{A}_2(\theta,\phi), j\boldsymbol{A}_2(\theta,\phi)] \tag{23}$$

Then the number of signals to be estimated of matrix $\boldsymbol{A}_{nc}(\theta,\phi)$ are equal to that of $\boldsymbol{A}_{nc}^{\mathrm{up}}(\theta,\phi)$, we rewrite $\boldsymbol{A}_{nc}^{\mathrm{up}}(\theta,\phi)$ as

$$\begin{aligned}&\boldsymbol{A}^{\mathrm{up}}(\theta,\phi)\\ &= \begin{bmatrix}[\boldsymbol{a}(\theta_1)\otimes\boldsymbol{a}_r(\phi_1), \cdots, \boldsymbol{a}_{t_1}(\theta_{K_{nc}})\otimes\boldsymbol{a}_r(\phi_{K_{nc}})]\boldsymbol{\Gamma},\\ [\boldsymbol{a}(\theta_{K_{nc}+1})\otimes\boldsymbol{a}_r(\phi_{K_{nc}+1}), \cdots, \boldsymbol{a}(\theta_K)\otimes\boldsymbol{a}_r(\phi_K)],\\ j[\boldsymbol{a}(\theta_{K_{nc}+1})\otimes\boldsymbol{a}_r(\phi_{K_{nc}+1}), \cdots, \boldsymbol{a}(\theta_K)\otimes\boldsymbol{a}_r(\phi_K)]\end{bmatrix}\end{aligned} \tag{24}$$

From the above equation, we can see that the number of columns of $\boldsymbol{A}^{\mathrm{up}}(\theta,\phi)$ are equals to $(K_{nc}+2K_c)$, whose angles are equal to:

$$\begin{aligned}&(\theta_1,\phi_1), \cdots, (\theta_{K_{nc}},\phi_{K_{nc}}), (\theta_{K_{nc}+1},\phi_{K_{nc}+1}), \cdots,\\ &\qquad (\theta_K,\phi_K), (\theta_{K_{nc}+1},\phi_{K_{nc}+1}), \cdots, (\theta_K,\phi_K).\end{aligned}$$

Then the signal subspace is consisted of $(K_{nc}+2K_c)$ eigenvectors corresponding to the largest $(K_{nc}+2K_c)$ eigenvalues of matrix $\hat{\boldsymbol{R}}$. Under no noise case, the signal subspace $\boldsymbol{E}_S$ and the steering matrix $\boldsymbol{A}_{nc}$ have the same space, that is, $\boldsymbol{E}_S = \boldsymbol{A}_{nc}\boldsymbol{T}$, where $\boldsymbol{T}$ is a nonsingular matrix. Substituting $\boldsymbol{E}_S = \boldsymbol{A}_{nc}\boldsymbol{T}$ into (21) and (22), one can get the following rotational invariant equations.

$$\boldsymbol{J}_2^\theta \boldsymbol{E}_S = \boldsymbol{J}_1^\theta \boldsymbol{E}_S \boldsymbol{\Psi}_\theta \tag{25}$$

$$\boldsymbol{J}_2^\phi \boldsymbol{E}_S = \boldsymbol{J}_1^\phi \boldsymbol{E}_S \boldsymbol{\Psi}_\phi \tag{26}$$

where $\boldsymbol{\Psi}_\theta = \boldsymbol{T}_\theta^{-1}\boldsymbol{\Phi}_\theta\boldsymbol{T}_\theta$ and $\boldsymbol{\Psi}_\phi = \boldsymbol{T}_\phi^{-1}\boldsymbol{\Phi}_\phi\boldsymbol{T}_\phi$. Eqs. (25) and (26) can be solved by the least squares (LS) or the total least squares (TLS) algorithm.

After eigendecomposition, the diagonal elements in $\boldsymbol{\Phi}_\theta$ and $\boldsymbol{\Phi}_\phi$ will be out-of-order. We need to find out the DOD and DOA estimation for a same target. Because there is no mismatch between the elements of $\boldsymbol{\Phi}_\theta$ and $\boldsymbol{\Phi}_\phi$, and its corresponding eigenvectors $\boldsymbol{T}_\theta$ and $\boldsymbol{T}_\phi$. Thus, different diagonal elements in $\boldsymbol{\Phi}_\theta$ and $\boldsymbol{\Phi}_\phi$ can be paired for the same source by pairing the orthogonal rows of $\boldsymbol{T}_\theta$ and $\boldsymbol{T}_\phi$. This pairing method is proposed by [20]. Let k denotes the row index of the matrix element with the largest absolute value in the fth column of the matrix $\{\boldsymbol{T}_\theta \cdot \boldsymbol{T}_\phi^{-1}\}$. Then the kth row of $\boldsymbol{T}_\theta$ must correspond to the fth row of $\boldsymbol{T}_\phi$. Now, the $\boldsymbol{\Phi}_\theta$ and $\boldsymbol{\Phi}_\phi$ have been correctly paired.

Now we can figure out the angle estimations of circular signals using the method of selecting the two closest estimations [18]. The residual estimations are noncircular signals' angle estimations. Detailed steps can be found in [18].

2) UNITARY ESPRIT

We extend the data matrix $\boldsymbol{Y}$ to $\boldsymbol{Z} = [\boldsymbol{Y}\boldsymbol{\Pi}_{2MN}\boldsymbol{Y}^*\boldsymbol{\Pi}_L]$. It doubles the snapshots from L to $2L$. Doubled snapshots data $\boldsymbol{Z}$ is transformed into real-valued matrix by using a sparse unitary matrix [21].

$$\boldsymbol{\Lambda} = \boldsymbol{Q}_{2MN}^H[\boldsymbol{Y}\boldsymbol{\Pi}_{2MN}\boldsymbol{Y}^*\boldsymbol{\Pi}_L]\boldsymbol{Q}_{2L} \in \mathbb{R}^{2MN\times 2L} \tag{27}$$

$\boldsymbol{Q}_o$ is a sparse unitary matrix, defined as

$$\begin{aligned}\boldsymbol{Q}_{2O} &= \frac{1}{\sqrt{2}}\begin{bmatrix}\mathrm{I}_O & j\mathrm{I}_O\\ \boldsymbol{\Pi}_O & -j\boldsymbol{\Pi}_O\end{bmatrix},\\ \boldsymbol{Q}_{2O+1} &= \frac{1}{\sqrt{2}}\begin{bmatrix}\mathrm{I}_O & \boldsymbol{0} & j\mathrm{I}_O\\ \boldsymbol{0}^T & \sqrt{2} & \boldsymbol{0}^T\\ \boldsymbol{\Pi}_O & \boldsymbol{0} & -j\boldsymbol{\Pi}_O\end{bmatrix}\end{aligned} \tag{28}$$

Then we calculate the real-valued covariance matrix $\hat{\boldsymbol{R}}_{\mathrm{real}} = 1/(2L)\boldsymbol{\Lambda}\boldsymbol{\Lambda}^H$. We can use the similar method of above ESPRIT to select the real-valued signal subspace $\boldsymbol{E}_S$. Then substituting $\boldsymbol{E}_S = \boldsymbol{A}_{nc}\boldsymbol{T}$ into (21) and (22), and then transforming the results into the real-valued form, one can get the

following rotational invariant equations (The detail can be found in [6]).

$$\boldsymbol{K}_2^{\theta}\boldsymbol{E}_S = \boldsymbol{K}_1^{\theta}\boldsymbol{E}_S\boldsymbol{\Theta}_{\theta} \tag{29}$$

$$\boldsymbol{K}_2^{\phi}\boldsymbol{E}_S = \boldsymbol{K}_1^{\phi}\boldsymbol{E}_S\boldsymbol{\Theta}_{\phi} \tag{30}$$

where $\boldsymbol{\Theta}_{\theta} = \boldsymbol{T}^{-1}\boldsymbol{\Omega}_{\theta}\boldsymbol{T}$ and $\boldsymbol{\Theta}_{\phi} = \boldsymbol{T}^{-1}\boldsymbol{\Omega}_{\phi}\boldsymbol{T}$. $\boldsymbol{K}_1^{\theta} = \mathrm{Re}\{\boldsymbol{Q}_{2(M-1)N}^H\boldsymbol{J}_2^{\theta}\boldsymbol{Q}_{2MN}\}$ and $\boldsymbol{K}_2^{\theta} = \mathrm{Im}\{\boldsymbol{Q}_{2(M-1)N}^H\boldsymbol{J}_2^{\theta}\boldsymbol{Q}_{2MN}\}$ are $2(M-1)N \times 2MN$ matrices.

$$\boldsymbol{\Omega}_{\theta} = \mathrm{diag}[\tan(\frac{\pi\sin\theta_1}{2}), \cdots, \tan(\frac{\pi\sin\theta_K}{2}), \tan(\frac{\pi\sin\theta_{K_{nc}+1}}{2}), \cdots, \tan(\frac{\pi\sin\theta_K}{2})]$$

is a real-valued matrix, which contains the desired DOD information. $\boldsymbol{K}_1^{\phi} = \mathrm{Re}\{\boldsymbol{Q}_{2M(N-1)}^H\boldsymbol{J}_2^{\phi}\boldsymbol{Q}_{2MN}\}$ and $\boldsymbol{K}_2^{\phi} = \mathrm{Im}\{\boldsymbol{Q}_{2M(N-1)}^H\boldsymbol{J}_2^{\phi}\boldsymbol{Q}_{2MN}\}$, and

$$\boldsymbol{\Omega}_{\phi} = \mathrm{diag}[\tan(\frac{\pi\sin\phi_1}{2}), \cdots, \tan(\frac{\pi\sin\phi_K}{2}), \tan(\frac{\pi\sin\phi_{K_{nc}+1}}{2}), \cdots, \tan(\frac{\pi\sin\phi_K}{2})]$$

is a real-valued matrix, which contains the desired DOA information. Eqs. (29) and (30) can be solved by the LS or TLS algorithm. Because $\boldsymbol{\Theta}_{\theta}$ and $\boldsymbol{\Theta}_{\phi}$ are real-valued. Therefore, we can use the following complex decomposition to achieve automatically pairing between the DODs and DOAs estimations [22].

$$\boldsymbol{\Theta}_{\theta} + j\boldsymbol{\Theta}_{\phi} = \boldsymbol{T}^{-1}\{\boldsymbol{\Omega}_{\theta} + j\boldsymbol{\Omega}_{\phi}\}\boldsymbol{T} \tag{31}$$

Then the paired DODs and DOAs estimations of $\{\theta_k, \phi_k\}$, $k = 1, \cdots, (K_{nc} + 2K_c)$ can be obtained by extracting the real and imaginary parts of the eigenvalues $\{\boldsymbol{\Omega}_{\theta} + j\boldsymbol{\Omega}_{\phi}\}$:

$$\begin{cases} \hat{\theta}_k = \arcsin\{2\arctan([\boldsymbol{\Omega}_{\theta}]_{kk})/\pi\} \\ \hat{\phi}_k = \arcsin\{2\arctan([\boldsymbol{\Omega}_{\phi}]_{kk})/\pi\} \end{cases}, \quad k = 1, \cdots, (K_{nc} + 2K_c) \tag{32}$$

We can use the above method to figure out K_c DOD and DOA estimations of circular signals. And the rest of the K_{nc} estimations are noncircular signals' ones.

C. IMPLEMENTATION AND REMARKS OF THE PROPOSED ALGORITHM

Based on the above theoretical analysis, the proposed DOD and DOA estimation with bistatic MIMO radar under the case of the coexistence noncircular and circular signals is summarized below. Here we take Unitary ESPRIT for an example.

Step 1 Perform matched filtering processing with Eq. (4), then perform vectorization operation with Eq. (5) to get a MN dimension received vector data $\boldsymbol{y}(t)$.

Step 2 Extend the received vector data $\boldsymbol{y}(t)$ to a $2MN$ dimension vector data $\boldsymbol{y}_{nc}(t)$ according to Eq. (11).

Step 3 Calculate the covariance matrix $\hat{\boldsymbol{R}}$ of $\boldsymbol{y}_{nc}(t)$, perform forward-backward covariance averaging to obtain the real-valued covariance matrix $\hat{\boldsymbol{R}}_{\mathrm{real}}$, then perform eigenvalue decomposition with $\hat{\boldsymbol{R}}_{\mathrm{real}}$ to obtain the $2MN \times (K_{nc} + 2K_c)$ dimension real-valued signal subspace $\boldsymbol{E}_S$.

Step 4 Construct the rotational invariant Eqs. (29) and (30) about signal subspace $\boldsymbol{E}_S$ using selection matrices, then solve them by means of LS or TLS to obtain rotational factor matrices $\boldsymbol{\Theta}_{\theta}$ and $\boldsymbol{\Theta}_{\phi}$.

Step 5 Pair the elements of $\boldsymbol{\Theta}_{\theta}$ and $\boldsymbol{\Theta}_{\phi}$ according to Eq. (31), then perform Eq. (32) to calculate the $(K_{nc}+2K_c)$ DOD and DOA estimations according to the paired elements of $\boldsymbol{\Theta}_{\theta}$ and $\boldsymbol{\Theta}_{\phi}$.

Step 6 Figure out the K_c pairs closest estimations, then average each pair to estimate angles of K_c circular signals, and the residual estimations are the angle estimations of K_{nc} noncircular signals.

Remark 1: The maximum number of detectable signals by our method is dependent on Eq. (11) and ESPRIT-like method. On the one hand, assume that the incident signals are uncorrelated with one another. Then the array covariance $\boldsymbol{R}$ matrix can be unwrapped as: $\boldsymbol{R} = \boldsymbol{A}_{nc}(\theta, \phi)\boldsymbol{R}_{ss}\boldsymbol{A}_{nc}(\theta, \phi)^H + \sigma_n^2\boldsymbol{I}_{2MN}$, where $\boldsymbol{R}_{ss} = \mathrm{diag}[\sigma_{s_1}^2, \cdots, \sigma_{s_K}^2, \sigma_{s_{Knc}}^2, \cdots, \sigma_{s_K}^2]$, $\sigma_{s_k}^2$ is the power of k incident signal. It is full rank, i.e. $\mathrm{rank}(\boldsymbol{R}_{ss}) = (K_{nc} + 2K_c)$. The array structure can be configured to ensure full column rank of $\boldsymbol{A}_{nc}(\theta, \phi)$. Then the maximum number of detectable signals depends on the maximum rank of $\boldsymbol{R}$, which is obviously equal to $\mathrm{rank}(\boldsymbol{R}) = 2MN$. So, $(K_{nc} + 2K_c) \leq 2MN$ should hold. On the other hand, using the ESRPIT-like method, DODs and DOAs are estimated from the signal subspace $\boldsymbol{E}_S$. From Eqs. (25) and (26), the row dimensions of $\boldsymbol{J}_2^{\theta}\boldsymbol{E}_S$ and $\boldsymbol{J}_2^{\phi}\boldsymbol{E}_S$ are equal to $2(M-1)N$ and $2M(N-1)$, respectively. Then the maximum number of detectable signals is $2\min[M(N-1), (M-1)N]$. Therefore, the maximum number of detectable signals for our proposed algorithm must satisfy

$$\begin{aligned}(K_{nc} + 2K_c) &\leq 2\min[MN, M(N-1), (M-1)N] \\ &= 2\min[M(N-1), (M-1)N].\end{aligned}$$

Remark 2: Note that our proposed algorithm needs to know the number of circular and noncircular signals as a priori. The result also has been pointed out by [23]. In active communication system, the number of signals and their forms are known to us, like BPSK (noncircular) or QPSK (circular), etc. So, we know the number of circular and noncircular signals.

V. DERIVATION OF THE Cramér-RAO BOUND (CRB)

It can be seen from the above analysis, the signal model is equivalent to that the signal we already know part information of the radar waveform. Therefore, it is reasonable to calculate the CRB by using the signal model $\boldsymbol{y}_{nc}(t) = \boldsymbol{A}_{nc}(\theta, \phi)\tilde{\boldsymbol{s}}(t) + \boldsymbol{n}_{nc}(t)$, which has utilized the noncircularity characteristic of noncircular signal already. Reference [24] gives a closed-form expression of the deterministic 1-D CRB. But in practice, the signals perhaps are Gaussian random distribution vectors with zero mean. And the parameters to be estimated are $\{\theta_k, \phi_k \,|k = 1, \cdots, K, (K_{nc} + 1), \cdots, K\}$.

Therefore, we gives a expression of the stochastic 2-D CRB in the following. The parameters can be rewritten as the vector form:

$$\begin{cases} \boldsymbol{\theta} = [\theta_1, \cdots, \theta_K, \theta_{(K_{nc}+1)}, \cdots, \theta_K] \\ \boldsymbol{\psi} = [\phi_1, \cdots, \phi_K, \phi_{(K_{nc}+1)}, \cdots, \phi_K] \end{cases} \tag{33}$$

It is well known that CRB is equal to the diagonal elements of inverse of Fisher information matrix (FIM). So we only calculate the FIM of parameters of Eq. (33), then the CRB can be obtained. In the following, the calculation of FIM is given. FIM can be expressed as

$$\boldsymbol{J} = \begin{bmatrix} \boldsymbol{J}_{\boldsymbol{\theta\theta}} & \boldsymbol{J}_{\boldsymbol{\theta\psi}} \\ \boldsymbol{J}_{\boldsymbol{\psi\theta}} & \boldsymbol{J}_{\boldsymbol{\psi\psi}} \end{bmatrix}_{2(K_{nc}+2K_c)\times 2(K_{nc}+2K_c)} \tag{34}$$

According to [25], the (i, j) elements of $\boldsymbol{J}_{\boldsymbol{hk}}$, $(\boldsymbol{h}, \boldsymbol{k} = \boldsymbol{\theta}, \boldsymbol{\psi})$ for L snapshots can be expressed as

$$\boldsymbol{J}_{\boldsymbol{hk}}(i, j) = L \cdot \mathrm{Tr}\left\{ \boldsymbol{R}^{-1} \frac{\partial \boldsymbol{R}}{\partial \boldsymbol{h}_i} \boldsymbol{R}^{-1} \frac{\partial \boldsymbol{R}}{\partial \boldsymbol{k}_j} \right\} \tag{35}$$

where $\boldsymbol{R}$ denotes virtual array covariance matrix. The array covariance $\boldsymbol{R}$ matrix can be unwrapped as

$$\boldsymbol{R} = \boldsymbol{A}_{nc}(\theta, \phi)\boldsymbol{R}_{ss}\boldsymbol{A}_{nc}(\theta, \phi)^H + \sigma_n^2 \boldsymbol{I}_{2MN} \tag{36}$$

Define the column vector of matrix $\boldsymbol{A}_{nc}(\theta, \phi)$ as $\boldsymbol{a}_{nc,k}$, according to Eq. (12), we can obtain that $\boldsymbol{a}_{nc,k}$ equals

$$\begin{cases} \boldsymbol{a}_{nc,k} = \begin{bmatrix} \boldsymbol{a}(\theta_k, \phi_k)\varepsilon_k \\ \boldsymbol{\Pi}_{MN}\boldsymbol{a}(\theta_k, \phi_k)^* \varepsilon_k^* \end{bmatrix}, & k = 1, \cdots, K_{nc} \\ \boldsymbol{a}_{nc,k} = \begin{bmatrix} \boldsymbol{a}(\theta_k, \phi_k) \\ \boldsymbol{\Pi}_{MN}\boldsymbol{a}(\theta_k, \phi_k)^* \end{bmatrix}, & k = K_{nc}+1, \cdots, K \\ \boldsymbol{a}_{nc,k} = \begin{bmatrix} \boldsymbol{a}(\theta_k, \phi_k) \\ j\boldsymbol{\Pi}_{MN}\boldsymbol{a}(\theta_k, \phi_k)^* \end{bmatrix}, & k = K+1, \cdots, (K_{nc}+2K_c) \end{cases} \tag{37}$$

Then we calculate the first-order partial derivatives of $\boldsymbol{R}$ with respect to θ_k and ϕ_k, as follows.

$$\frac{\partial \boldsymbol{R}}{\partial \xi_k} = \frac{\sigma_{s_k}^2 \partial(\boldsymbol{a}_{nc,k}\boldsymbol{a}_{nc,k}^H)}{\partial \xi_k} = \sigma_{s_k}^2 \frac{\partial \boldsymbol{a}_{nc,k}}{\partial \xi_k}\boldsymbol{a}_{nc,k}^H + \sigma_{s_k}^2 \boldsymbol{a}_{nc,k}\frac{\partial \boldsymbol{a}_{nc,k}^H}{\partial \xi_k} \tag{38}$$

where ξ denotes θ, ϕ. The results of (38) in detail are given in the following. For simplicity, $\boldsymbol{a}_t(\theta_k)$ and $\boldsymbol{a}_r(\phi_k)$ are marked with $\boldsymbol{a}_{t,k}$ and $\boldsymbol{a}_{r,k}$, respectively. Equation (39), (40) as shown at the bottom of this page.
where

$$\boldsymbol{c}_{t,k} = j\pi[0, \cos\theta_k, \cdots, (M-1)\cos\theta_k)]^T \tag{41}$$

$$\boldsymbol{c}_{r,k} = j\pi[0, \cos\phi_k, \cdots, (N-1)\cos\phi_k)]^T \tag{42}$$

VI. COMPUTER SIMULATIONS

In this section, computer simulation results are used to prove the effectiveness of the proposed algorithm. The root mean square error (RMSE) of angle estimation is defined as $\mathrm{RMSE} = \sqrt{\frac{1}{KQ}\sum_{q=1}^{Q}\sum_{k=1}^{K}(\hat{\zeta}_{k,q} - \zeta_k)^2}$, where Q is Monte Carlo experiments and $\zeta = \theta, \phi$. In following simulations, we set that the noncircular incident signals are consisted of BPSK signals and the circular incident signals are consisted of QPSK signals. Our proposed algorithms in the following figures are marked with C-NC ESPRIT and C-NC Unitary ESPRIT.

In the first experiment, we consider a bistatic MIMO radar system with $M = 6$ and $N = 6$. We set there are $K = 3$ uncorrelated incident signals, in which there has $K_{nc} = 1$ noncircular source and $K_c = 2$ circular sources. The DOD and DOA of noncircular source equals $\theta_1 = [10°]$ and $\phi_1 = [-50°]$, respectively, and its rotation phase equals $\frac{2\pi}{5}$. The DOD and DOA of circular sources equal $[\theta_2, \theta_3] = [20°, 30°]$ and $[\phi_2, \phi_3] = [-30°, -10°]$. We set SNR = 20dB and the number of snapshots is $L = 100$. Table 1 gives the DOD and

$$\frac{\partial \boldsymbol{a}_{nc,k}}{\partial \theta_k} = \begin{cases} \begin{bmatrix} (\boldsymbol{c}_{t,k} \odot \boldsymbol{a}_{t,k}) \otimes \boldsymbol{a}_{r,k}\varepsilon_k \\ \boldsymbol{\Pi}_{MN}[(\boldsymbol{c}_{t,k} \odot \boldsymbol{a}_{t,k}) \otimes \boldsymbol{a}_{r,k}]\varepsilon_k^* \end{bmatrix}, & k = 1, \cdots, K_{nc} \\ \begin{bmatrix} (\boldsymbol{c}_{t,k} \odot \boldsymbol{a}_{t,k}) \otimes \boldsymbol{a}_{r,k} \\ \boldsymbol{\Pi}_{MN}[(\boldsymbol{c}_{t,k} \odot \boldsymbol{a}_{t,k}) \otimes \boldsymbol{a}_{r,k}]^* \end{bmatrix}, & k = K_{nc}+1, \cdots, K \\ \begin{bmatrix} (\boldsymbol{c}_{t,k} \odot \boldsymbol{a}_{t,k}) \otimes \boldsymbol{a}_{r,k} \\ j\boldsymbol{\Pi}_{MN}[(\boldsymbol{c}_{t,k} \odot \boldsymbol{a}_{t,k}) \otimes \boldsymbol{a}_{r,k}]^* \end{bmatrix}, & k = K+1, \cdots, (K_{nc}+2K_c) \end{cases} \tag{39}$$

$$\frac{\partial \boldsymbol{a}_{nc,k}}{\partial \phi_k} = \begin{cases} \begin{bmatrix} \boldsymbol{a}_{t,k} \otimes (\boldsymbol{c}_{r,k} \odot \boldsymbol{a}_{r,k})\varepsilon_k \\ \boldsymbol{\Pi}_{MN}\boldsymbol{a}_{t,k} \otimes [(\boldsymbol{c}_{r,k} \odot \boldsymbol{a}_{r,k})]\varepsilon_k^* \end{bmatrix}, & k = 1, \cdots, K_{nc} \\ \begin{bmatrix} \boldsymbol{a}_{t,k} \otimes (\boldsymbol{c}_{r,k} \odot \boldsymbol{a}_{r,k}) \\ \boldsymbol{\Pi}_{MN}\boldsymbol{a}_{t,k} \otimes [(\boldsymbol{c}_{r,k} \odot \boldsymbol{a}_{r,k})]^* \end{bmatrix}, & k = K_{nc}+1, \cdots, K \\ \begin{bmatrix} \boldsymbol{a}_{t,k} \otimes (\boldsymbol{c}_{r,k} \odot \boldsymbol{a}_{r,k}) \\ j\boldsymbol{\Pi}_{MN}\boldsymbol{a}_{t,k} \otimes [(\boldsymbol{c}_{r,k} \odot \boldsymbol{a}_{r,k})]^* \end{bmatrix}, & k = K+1, \cdots, (K_{nc}+2K_c) \end{cases} \tag{40}$$

TABLE 1. The angle estimation results before averaging.

Method	Angle	Noncircular source	Circular source #1		Circular source #2	
C-NC ESPRIT	DOD	10.002	20.010	20.010	29.975	30.016
	DOA	-49.996	-30.009	-30.009	-10.009	-9.991
C-NC Unitary ESPRIT	DOD	9.981	30.002	30.007	19.996	20.007
	DOA	-50.000	-9.995	-9.9901	-30.024	-29.992

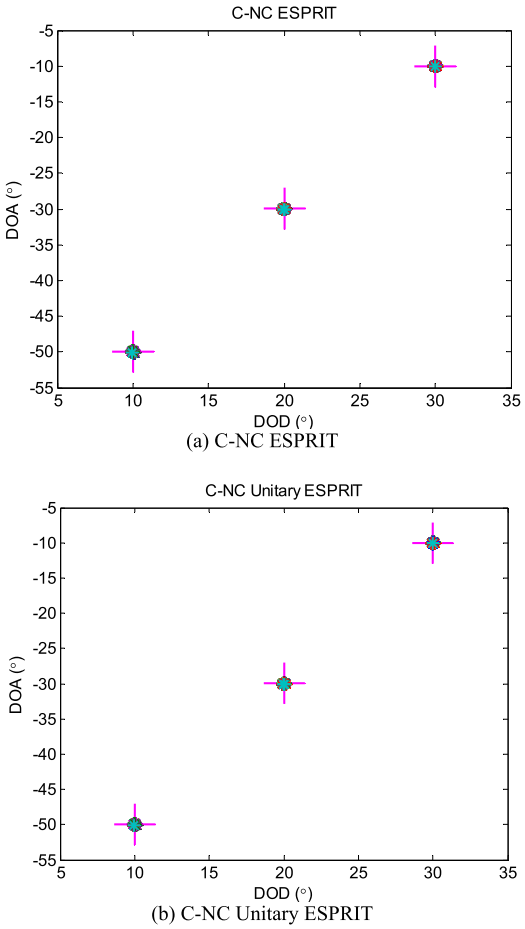

(a) C-NC ESPRIT

(b) C-NC Unitary ESPRIT

FIGURE 1. The estimations of three incident signals with 100 runs and $M = 6$, $N = 6$, SNR = 20 dB, $L = 100$. (a) C-NC ESPRIT. (b) C-NC Unitary ESPRIT.

DOA estimations before averaging the closed angles of the circular sources with one trial. It is five estimations, which has the same number with theoretical analysis$K_{nc}+2K_c = 5$. Figs. 1 (a) and (b) show the paired angles estimation results with 100 Monte Carlo trials. It is indicated in the figures that the DODs and DOAs of the three incident signals are well localized and paired correctly.

In the second experiment, we verify the advantage on the more number of detectable targets of our proposed algorithm. Here we set that $M = 2, N = 4$ in the bistatic MIMO radar. The maximum number of localizable targets are four using the ESPRIT algorithm in [5] and Unitary ESPRIT in [6], both of the two methods doesn't exploit the noncircularity characteristic. Therefore, we set five targets in the simulations,

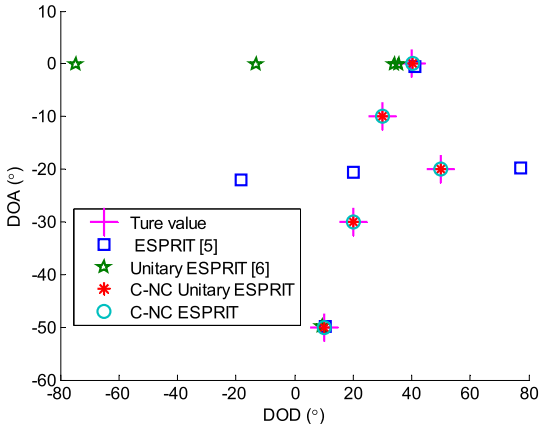

FIGURE 2. The estimation results of five targets $M = 2$, $N = 4$, SNR = 20 dB.

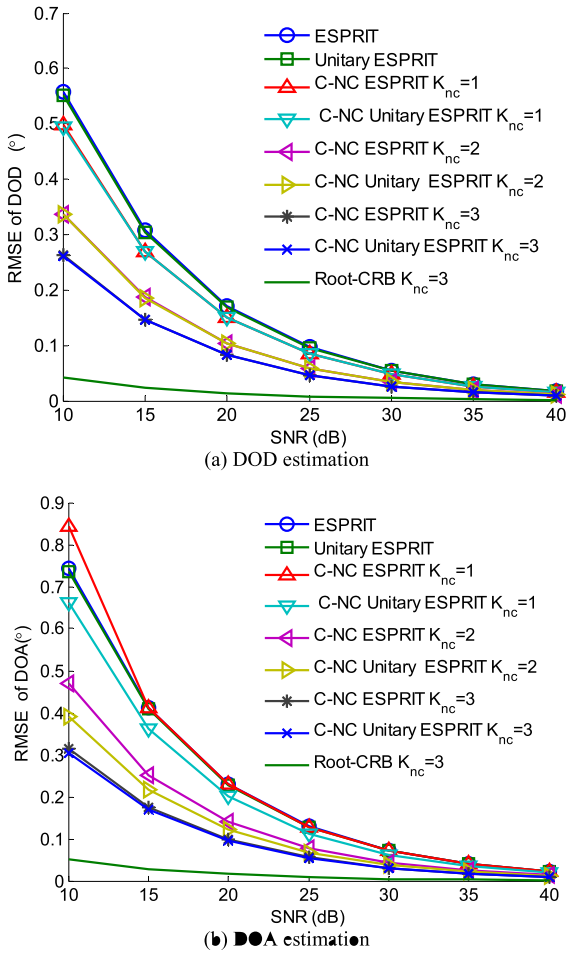

(a) DOD estimation

(b) DOA estimation

FIGURE 3. RMSE versus SNR with $M = 4$, $N = 4$, $L = 50$, $K = 4$ and 1000 Monte Carlo trials. (a) DOD estimation. (b) DOA estimation.

which have four noncircular signals and one circular signal. Then $K_{nc} + 2K_c = 6$ and $2\min[M(N-1), (M-1)N] = 8$. Thus, the methods in [5] and [6] will fail but our proposed method will success in the theoretical analysis. Fig. 2 gives the estimation results of five targets with $M = 2$ and $N = 4$

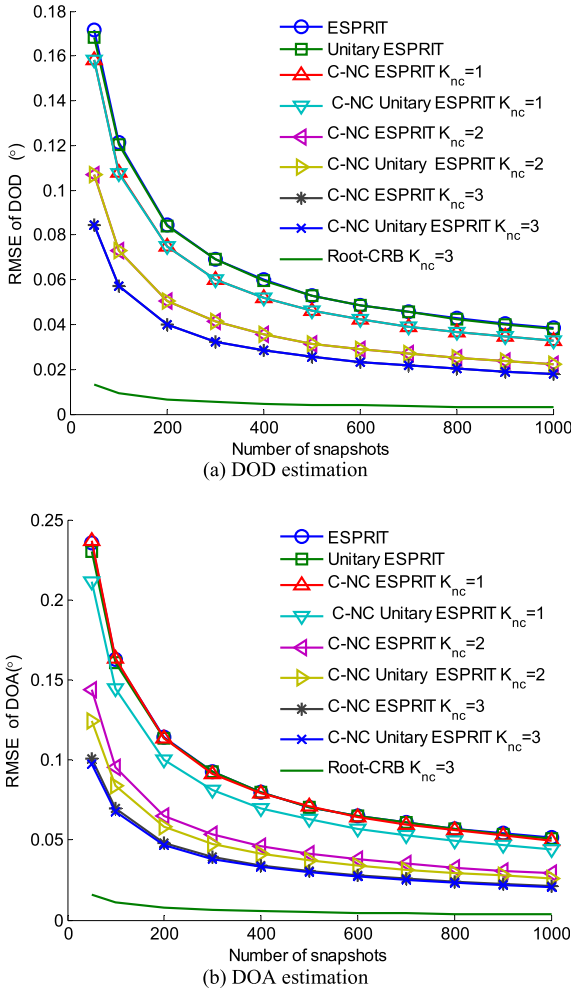

FIGURE 4. RMSE versus the number of snapshots with $M = 4$, $N = 4$, SNR $= 20$, $K = 4$ and 1000 Monte Carlo trials. (a) DOD estimation. (b) DOA estimation.

by using the methods in [5] and [6], and our proposed method. It can be seen from the figure that the results are as what we expected.

Figs. 3 (a) and (b) illustrate the RMSE versus SNR, also compared with the methods in [5] and in [6]. In the third experiment, we set that $M = 2$, $N = 4$ in the bistatic MIMO radar. The number of uncorrelated incident signals is $K = 4$, in which the angles equal $\theta = [10°, 20°, 30°, 40°]$ and $\phi = [-50°, -30°, -10°, 0°]$. The number of noncircular signals is set as from $K_{nc} = 1$ up to $K_{nc} = 3$. The rotational phases are set as starting from zero with $\frac{\pi}{4}$ spacing. We set the snapshots equal $L = 50$ Monte Carlo trials are 1000. It is indicated in the figures that the angle estimation performance of the proposed algorithms are better than those of the methods in [5] and in [6]. In addition, the more the number of noncircular signals are, the better angle estimation performance will be. Because the more number of noncircular signals are, the less number of signals to be estimated in (11) will be.

Figs. 4 (a) and (b) show the RMSE versus the number of snapshots, compared with the methods in [5] and in [6]. In the last experiment, we set SNR $= 20$dB and the others simulation conditions are the same as the above simulation ones. It is indicated in Figs. 4 (a) and (b) that the performance of DOD and DOA estimation of the proposed algorithm becomes better in collaboration with L increasing and outperforms the methods in [5] and in [6]. In addition, the more the number of noncircular signals are, the better angle estimation performance will be. The reason is same as the Fig. 3.

VII. CONCLUSIONS

The problem of joint DOD and DOA estimation with bistatic MIMO radar under the case of the coexistence of circular and noncircular signals has studied in this paper. First, the signal model is modified to the new signal model, which incident signals are noncircular. Then, the rotational invariance of doubled array, which makes full use of noncircularity characteristic of noncircular signal, is figured out. Last, the DOD and DOA are estimated by the methods of ESPRIT and Unitary ESPRIT algorithm. From the simulation results, we can see that the proposed algorithm has the three advantages: 1) it has better angle estimation accuracy than that of conventional method, which does not use the noncircularity characteristic; 2) it has more number of detectable incident signals; 3) when the number of whole incident signals is constant, the more number of noncircular signals, the higher angle estimation accuracy will be. Note that our proposed algorithm needs to know the number of circular and noncircular signals as a priori.

Acknowledgment

This work was presented at the Proceedings of the IEEE Radar Conference, Philadelphia, PA, USA, 2–6 May 2016.

REFERENCES

[1] E. Fishler, A. Haimovich, R. Blum, D. Chizhik, L. Cimini, and R. Valenzuela, "MIMO radar: An idea whose time has come," in *Proc. IEEE Radar Conf.*, Philadelphia, PA, USA, Apr. 2004, pp. 71–78.

[2] I. Bekkerman and J. Tabrikian, "Target detection and localization using MIMO radars and sonars," *IEEE Trans. Signal Process.*, vol. 54, no. 10, pp. 3873–3883, Oct. 2006.

[3] J. Li and P. Stoica, "MIMO radar with colocated antennas," *IEEE Signal Process. Mag.*, vol. 24, no. 5, pp. 106–114, Sep. 2007.

[4] L. Xu, J. Li, and P. Stoica, "Target detection and parameter estimation for MIMO radar systems," *IEEE Trans. Aerosp. Electron. Syst.*, vol. 44, no. 3, pp. 927–939, Jul. 2008.

[5] C. Duofang, C. Baixiao, and Q. Guodong, "Angle estimation using ESPRIT in MIMO radar," *Electron. Lett.*, vol. 44, no. 12, pp. 770–771, Jun. 2008.

[6] G. Zheng, B. Chen, and M. Yang, "Unitary ESPRIT algorithm for bistatic MIMO radar," *Electron. Lett.*, vol. 48, no. 3, pp. 179–181, 2012.

[7] X. Zhang *et al.*, "Direction of departure (DOD) and direction of arrival (DOA) estimation in MIMO radar with reduced-dimension MUSIC," *IEEE Commun. Lett.*, vol. 14, no. 12, pp. 1161–1163, Dec. 2010.

[8] M. L. Bencheikh and Y. Wang, "Joint DOD-DOA estimation using combined ESPRIT-MUSIC approach in MIMO radar," *Electron. Lett.*, vol. 46, no. 15, pp. 1081–1083, 2010.

[9] B. Tang, J. Tang, Y. Zhang, and Z. Zheng, "Maximum likelihood estimation of DOD and DOA for bistatic MIMO radar," *Signal Process.*, vol. 93, no. 5, pp. 1349–1357, 2013.

[10] X. Zhang, Z. Xu, L. Xu, and D. Xu, "Trilinear decomposition-based transmit angle and receive angle estimation for multiple-input multiple-output radar," *IET Radar Sonar Navigat.*, vol. 5, no. 6, pp. 626–631, 2011.

[11] X. Wang, W. Wang, X. Li, and J. Liu, "Real-valued covariance vector sparsity-inducing DOA estimation for monostatic MIMO radar," *Sensors*, vol. 15, no. 11, pp. 28271–28286, 2015.
[12] J. Li, X. Zhang, R. Cao, and M. Zhou, "Reduced-dimension MUSIC for angle and array gain-phase error estimation in bistatic MIMO radar," *IEEE Commun. Lett.*, vol. 17, no. 3, pp. 443–446, Mar. 2013.
[13] M. L. Yang, B. X. Chen, and X. Y. Yang, "Conjugate ESPRIT algorithm for bistatic MIMO radar," *Electron. Lett.*, vol. 46, no. 5, pp. 1692–1694, 2011.
[14] M. L. Bencheikh and Y. Wang, "Non circular ESPRIT-Root MUSIC joint DOA-DOD estimation in bistatic MIMO radar," in *Proc. 7th Int. Workshop Syst., Signal Process. Appl. (WOSSPA)*, 2011, pp. 51–54.
[15] W. Wang, X. Wang, H. Song, and Y. Ma, "Conjugate ESPRIT for DOA estimation in monostatic MIMO radar," *Signal Process.*, vol. 93, no. 7, pp. 2070–2075, 2013.
[16] X. Wang, W. Wang, and D. Xu, "Low-complexity ESPRIT-root-MUSIC algorithm for non-circular source in bistatic MIMO radar," *Circuits Syst. Signal Process.*, vol. 34, no. 4, pp. 1265–1278, 2014.
[17] X. Wang *et al.*, "Sparsity-aware DOA estimation scheme for noncircular source in MIMO radar," *Sensors*, vol. 16, no. 4, p. 539, 2016.
[18] J. Steinwandt, F. Roemer, and M. Haardt, "Esprit-type algorithms for a received mixture of circular and strictly non-circular signals," in *Proc. IEEE Int. Conf. Acoust., Speech Signal Process. (ICASSP)*, Apr. 2015, pp. 2809–2813.
[19] X. Yang, G. Zheng, and J. Tang, "ESPRIT algorithm for coexistence of circular and noncircular signals in bistatic MIMO radar," in *Proc. IEEE Radar Conf. (RadarConf)*, Philadelphia, PA, USA, May 2016, pp. 1–4.
[20] K. T. Wong and M. D. Zoltowski, "Closed-form direction finding and polarization estimation with arbitrarily spaced electromagnetic vector-sensors at unknown locations," *IEEE Trans. Antennas Propag.*, vol. 48, no. 5, pp. 671–681, May 2000.
[21] M. Haardt and J. A. Nossek, "Unitary ESPRIT: How to obtain increased estimation accuracy with a reduced computational burden," *IEEE Trans. Signal Process.*, vol. 43, no. 5, pp. 1232–1242, May 1995.
[22] M. D. Zoltowski, M. Haardt, and C. P. Mathews, "Closed-form 2-D angle estimation with rectangular arrays in element space or beamspace via unitary ESPRIT," *IEEE Trans. Signal Process.*, vol. 44, no. 2, pp. 316–328, Feb. 1996.
[23] F. Gao, A. Nallanathan, and Y. Wang, "Improved MUSIC under the coexistence of both circular and noncircular sources," *IEEE Trans. Signal Process.*, vol. 56, no. 7, pp. 3033–3038, Jul. 2008.
[24] J. Steinwandt, F. Roemer, and M. Hardt, "Deterministic Cramér-Rao bound for a mixture of circular and strictly noncircular signals," in *Proc. ISWCS*, Aug. 2015, pp. 661–665.
[25] H. L. Trees, *Detection, Estimation, and Modulation Theory, Part IV: Optimum Array Processing*. New York, NY, USA: Wiley, 2002.

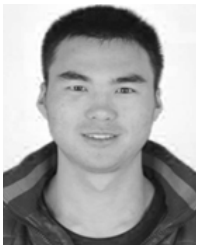

GUIMEI ZHENG (S'16) was born in Fujian, China, in 1987. He received the B.Eng. degree in biomedical engineering and the Ph.D. degree in signal and information processing from Xidian University, China, in 2009 and 2014, respectively. He is currently a full-time Post-Doctoral Research Fellow with the Department of Electronic Engineering, Tsinghua University, Beijing, China.

His research interests lie in MIMO radar and vector sensor array signal processing.

JUN TANG (M'08) was born in Jiangsu, China, in 1973. He received the Ph.D. degree in electronic engineering from Tsinghua University, Beijing, China, in 2000. He is currently a Full Professor with the Department of Electronic Engineering, Tsinghua University.

His research interests include array signal processing, information theory, and MIMO radar.

XUAN YANG was born in Yunnan, China, in 1990. He received the B.S. degree from the Central University of Finance and Economics, in 2014. He is currently pursuing the master's degree with the Department of Electronic Engineering, Tsinghua University.

His research interests include array signal processing and MIMO radar.